Optoacoustic Sensor for Nanoparticle Linked Immunosorbent Assay (NanoLISA)

André Conjusteau[(1)], Anton Liopo[(1)], Dmitri Tsyboulski[(1)], Sergey A. Ermilov[(1)], William R. Elliott III[(2)], Norman Barsalou[(2)], Saher M. Maswadi[(3)], Randolph D. Glickman[(3)], and Alexander A. Oraevsky[(1,*)]

(1) Tomowave Laboratories, Houston, TX 77057
(2) Naval Health Research Ctr. Detachment Brooks City-Base, 78235
(3) The Univ. of Texas Health Science Ctr. at San Antonio, TX 78229

ABSTRACT

We developed an optoacoustic biosensor intended for the detection of bloodborne microorganisms using immunoaffinity reactions of antibody-coupled gold nanorods as contrast agents specifically targeted to the antigen of interest. Optoacoustic responses generated by the samples are detected using a wide band ultrasonic transducer. The sensitivity of the technique has been assessed by determining minimally detectable optical density which corresponds to the minimum detectable concentration of the target viral surface antigens. Both ionic solutions and gold nanorods served as the contrast agent generating the optoacoustic response. The sensitivity of Nano-LISA is at least OD=10^{-6} which allows reliable detection of 1 pg/ml (depending on the commercial antibodies that are used). Adequate detection sensitivity, as well as lack of non-specific cross-reaction between antigens favors NanoLISA as a viable technology for biosensor development.

Key words: NanoLISA, gold nanoparticle conjugates, optoacoustic detection, specific binding, contrast agents.

INTRODUCTION

The threat of contaminants such as bacterial, viral, and chemical toxins has long been recognized as a public health hazard. For instance, infectious keratitis is a major cause of visual disability and blindness; infections due to herpes simplex virus (HSV) are some of the most common and difficult to diagnose. In order to treat this condition effectively, rapid identification of the responsible infectious agent must occur to deliver specific and timely treatment. The current diagnostic standard involves microbiological culturing and requires several days; improper management can lead to marked loss of vision[1]. Additionally, the cultures' yields are often too low for a conclusive diagnosis and treatment specificity has to be sacrificed.

Sensitive methods exist for detecting most pathogens of concern, utilizing a number of technologies, e.g. isolation of target nucleic acids (with PCR amplification if necessary[2,3]) or immunological-based ELISA or affinity assays[4,5]. These tests form the foundation of a variety of clinical microbiological assays. Our work on NanoLISA will build on this foundation by developing a new technology utilizing pulsed radiation optoacoustic spectroscopy for the detection of immunoaffinity complexes[6-9]. The advantage of optoacoustic detection is that it offers greater sensitivity compared to existing methodologies, such as linked colorimetric reactions or fluorescence. Furthermore, it is the only viable method of detection when studying heavily light-scattering samples.

(*) Alexander A. Oraevsky, aao@tomowave.com, www.tomowave.com

Photons Plus Ultrasound: Imaging and Sensing 2011, edited by Alexander A. Oraevsky, Lihong V. Wang,
Proc. of SPIE Vol. 7899, 789910 · © 2011 SPIE · CCC code: 1605-7422/11/$18 · doi: 10.1117/12.879401

The principle of optoacoustic detection relies on the occurrence of thermal confinement which happens when the laser pulse duration is small compared to the transit time of sound through the penetration depth of the light. In this case, instantaneous heating of the medium can be assumed. Since the density of the medium cannot change substantially during laser pulse action, a stress field is created as a result of the inhomogeneous temperature field, and an acoustic signal is generated. As light absorption dictates the amount of energy absorbed in the sample, the resulting pressure wave will vary in amplitude depending on the analyte's optical properties.

Published results have shown that gold nanorods (GNR), being the size of a cluster of a few large protein molecules (roughly 15x50 nm), can absorb light about one thousand times more strongly than an equivalent volume of an organic dye[10,11]. The optoacoustic efficiency of these contrast agents is also due to the localized superheating of the particles. As they are unable to release energy in the form of photoluminescence, superheating results in evaporation of a nanolayer of surrounding water[10,12], which produces acoustic waves up to an order of magnitude stronger than that from a homogeneously absorbing solution with equal average absorption coefficient[13]. At TomoWave Laboratories, we manufacture particles[14] with an extinction coefficient around 4×10^9 $M^{-1}cm^{-1}$. Recent studies demonstrated an optoacoustic limit of detection of 10^7 particles per ml for gold nanorods[15,16]. This compares very favorably to fluorescence detection, where the practical detection limit with commercial instrumentation is $\sim10^{-11}$ M of highly fluorescent fluorophores (equivalent to approximately 10^9 molecules/ml)[17]. We have shown in a breast cancer cell culture that gold NPs could be effectively conjugated to antibodies raised against various protein receptors expressed in high concentration in malignant breast tumors[18]. Such conjugation is based on a very strong affinity of molecular sulfur atoms to the gold surface, allowing chemical (covalent) bonding between the gold and the ligand. Additionally, we have shown those covalently conjugated gold nanorods to be stable for hours in blood, thereby demonstrating their stability *in situ*[18].

EXPERIMENTAL

GNR Fabrication

Presented below are the details of our GNR fabrication protocol adapted from previously reported methodology[19,20]. The base procedure is tailored to the needs of the specific experiments presented in this paper. It allows high-yield fabrication of a narrow size distribution of rods with a 755 nm plasmon resonance. The details of the procedure have been published elsewhere[14,18] and only the generalities of the method will be summarized. A gold seed solution is first prepared by mixing solutions of gold salts, surfactant (CTAB) and a strong reducing agent ($NaBH_4$). Seeds about 2 nm in diameter start to form immediately after mixing, and the solution is usually used within 2-4 hours. Subsequently, a growth solution is made by mixing the surfactant (CTAB), gold salt, and silver nitrate solutions in the order presented. Ascorbic acid is added to the resulting brown-yellow solution which immediately turns colorless, indicating a change in the oxidation state of the gold ions present. Then, an aliquot of seed solution is added to the growth solution, the mixture is gently mixed by inversion and the reaction is brought to completion over 24 hours in thermostatic conditions at 30°C.

Before covalent binding with polyethylene glycol (PEG), or conjugation with a monoclonal antibody (mAb), the GNR were centrifuged at low speed (4000 rpm, 10 min) for separation (and subsequent removal) of other aggregates (platelets, stars). The pellet was removed and for the next steps, only the supernatant fraction was used. For Pegylation[18,21] the GNR solution was centrifuged at 14000 g for 10 minutes, the supernatant was removed, and the pellet was resuspended in deionized (DI) water to reduce CTAB concentration to 0.01 M. Then, 0.1 ml of 2 mM potassium carbonate (K_2CO_3) was added to 1 ml of aqueous GNR solution and 0.1 ml of 0.1 mM mPEG-Thiol-5000 (Laysan Bio Inc., Arab, AL). The resulting mixture was kept on a rocking platform at room temperature overnight.

Excess mPEG thiol was removed from solution by two rounds of centrifugation and final resuspension in PBS (pH 7.4).

A protocol for conjugation of GNR has been developed at TomoWave Laboratories. It replaces CTAB as was described before[18,22] on the surface of gold nanorods with Nanothink-16 and polyethyleneglycol, and the desired monoclonal antibody. Specifically, one mL of GNR solution (coated with CTAB) was centrifuged twice in a 1.5 mL Eppendorf tube at 14000 RPM for 10 minutes and resuspended in one mL of Milli-Q water (MQW) to a concentration of 1 nM. Then, 10 μL of 5 mM Nanothinks acid16 (Sigma) in ethanol was added to the GNR solution, and the solution was sonicated for 30 minutes at 50°C to prevent aggregation. The solution was centrifuged at 12000 RPM for 10 minutes, the supernatant was removed and the pellet was resuspended in MQW. 10 μL of 1-ethyl-3-[3-imethylaminopropyl] carbodiimide hydrochloride (EDC, Pierce) and sulfo-NHS (Pierce) was added from stock solution in 2-(4-Morpholino)ethane Sulfonic Acid (MES) buffer in 10 mM and 0.4 mM, respectively. The mixture was sonicated for 30 minutes at room temperature to produce activated GNR (i.e. GNR that are capable of binding to the amine side chain of proteins). Commercial purified mAb was then added to a final concentration of 25 μg/mL to 1 mL of 1 nM activated GNR. The mixture was sonicated at room temperature for 1 hour and then left on a rocking platform overnight. Following the removal of excess mAb, 10 μL of PEG-Thiol (1 mM) was added to 1 mL of GNR-mAb conjugates, and the mixture was incubated at room temperature for 12 h. The solution of GNR-mAb-PEG conjugate was centrifuged at 12000 g for 10 minutes, the supernatant was removed and the pellet was resuspended in PBS pH 7.4 to a concentration of 1 nM (or optical density around 4.0 as measured by Beckman 530 and Thermo Scientific Evolution 201 Spectrophotometer).

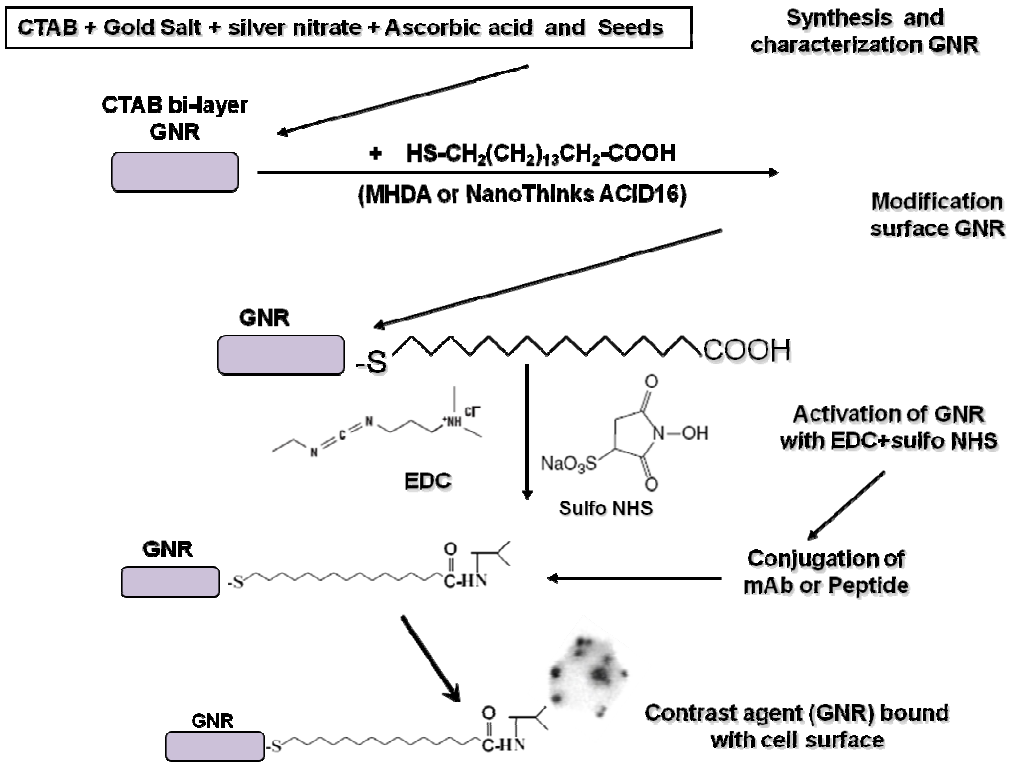

Figure 1. Road map of GNR fabrication and mAb conjugation. See text and cited references for details.

Detection Scheme

A fully functional prototype of an optoacoustic spectrometer, using a tunable titanium sapphire laser as the excitation source, has already been implemented at TomoWave Laboratories. Our laser delivers up to 100 mJ per 12 ns pulse of 760 nm radiation, at a repetition rate of 10 Hz. The laser is outfitted with polarizing optics on output permitting continuous variation of the output energy. In the work presented, the output of the laser is significantly attenuated, and only a small fraction of the 9 mm diameter beam is coupled to the experiment with a 2 mm diameter fiber bundle. Therefore, less than 500 µJ per pulse reach the sample.

An illustration of the latest version of the detector is presented below (Fig. 2). It features a deceptively simple direct illumination scheme where pulsed radiation is applied directly through the sample, towards the detector. The sound waves are transduced into electrical signal by a small piece of piezoelectric polyvinylidene difluoride (PVDF). The PVDF film is sitting atop an electrically conductive brass chuck acting both as backing material and signal contact. Through careful use of acrylic spacers acting as acoustic delay lines, the intense signal originating from the light impulse can be separated from that of the sample under study. Furthermore, this scheme showed highly efficient suppression of PVDF's intense pyroelectric character with judicious use of metalized film placed in between the delay lines.

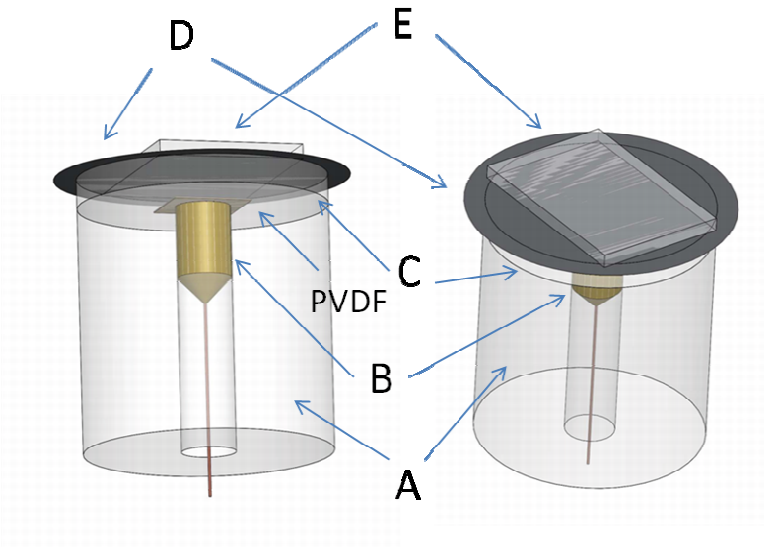

Figure 2. Experimental setup. A) acrylic body, B) brass backing used as signal electrical contact, C) light signal delay line (3 mm acrylic), D) light shield (metallized Mylar), and E) sample signal delay line (1.5 mm acrylic). Not shown is a 25 micron copper film, located between the square PVDF element and the light signal delay line, used as ground electrode. The entire body of the detector is also wrapped in copper foil (connected to ground) for electromagnetic shielding purposes.

With this setup, a small volume (6 µl) of the solution under investigation is placed upon the top of the detector's second delay line and covered with a microscope cover slip in order to spread evenly across the whole area of the device. Knowing both the volume and dimension of the top piece of acrylic, we can calculate we generate an 18 µm thick sample. The sample is illuminated from the output of a 2 mm optical fiber bundle and the spot size at the detector is about 3mm in diameter. The laser energy is adjusted to 300 µJ per pulse at the output of the fiber: the excitation fluence is therefore 4 mJ/cm^2. The signal is amplified via a custom-built, two-stage, high input impedance device delivering 17 dB of gain before being read directly into a digitizing oscilloscope operating at a sampling rate of 1.25 GHz. The signal quality is partly limited by electrical noise pick-up at about 0.05 mV_{RMS}. In the case of solid

samples, for instance substances adsorbed onto glass or acrylic substrates, a thin layer of DI water is used as acoustic couplant and the substrate is simply laid on top of the detector, sample side down (i.e. towards the detector).

RESULTS AND DISCUSSION

Analysis of Signals

Results pertaining to experiments related to the current study have already been presented in the literature[23,24]. An interesting facet of these experiments is the rather limited frequency content of the acquired signals. In particular, a very high frequency optoacoustic transducer (LiNBO-based, 100 MHz center frequency) was used in parallel with a beam deflection scheme using a fast split photodiode. For both detection methods, Fourier analysis of the collected impulses reported the acoustic information was contained in a very limited frequency band. In fact, little signal energy was found above 10 MHz. This observation justifies the use of rather modest detection bandwidth: noise is kept to a minimum and readily available PVDF film can be used, therefore permitting flexibility in design and geometry. The proposed delay-line-based scheme is further justified in the low frequencies expected, as acrylic acts as an acoustic absorber at high-frequencies (roughly 6dB/cm at 5 MHz).

Ionic Solutions: $NiSO_4$

In a first series of tests, the optoacoustic response of several $NiSO_4$ solutions was measured. The solutions had absorptivities (μ_a) of 0.22, 0.44, 0.83, 1.6 and 3.2cm^{-1}, as measured with a Beckman DU500 spectrophotometer. Deionized water was also measured for control, and blank scans were acquired and used to perform background subtraction in order to remove the intrinsic instrument response. The resulting signals are shown below, in panel A) of figure 3.

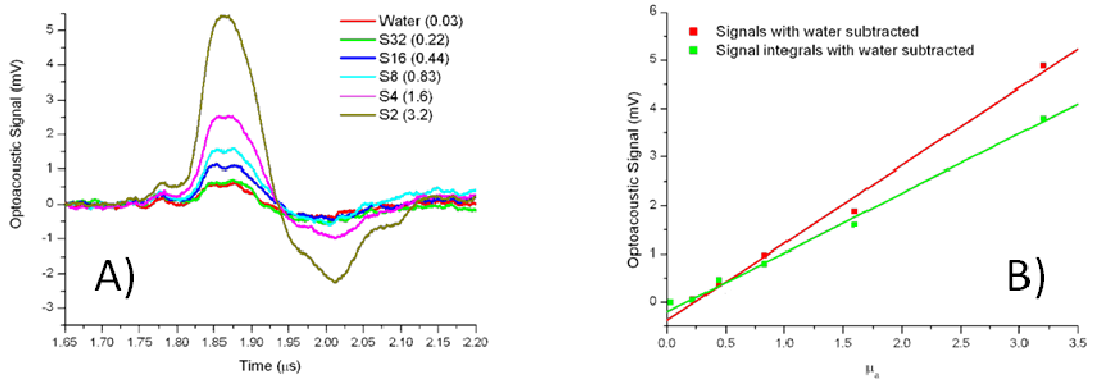

Figure 3. A) Processed optoacoustic signals. B) Limit of detection obtained from ionic solutions of NiSO4.

Due to the intense light signal sensed at the metalized film, the comparatively small optoacoustic signals emanating from the samples were riding on a sloping background. Subtracting background signals obtained solely from light impact allowed for straightening the baseline, therefore simplifying the analysis of both amplitudes and integrals. The dependence of both properties upon variation of optical density is plotted in panel B) of Fig. 3. In both cases, only the positive part of the signal is considered, as the negative overshoot is significantly distorted by acoustic differentiation and other geometric effects[25]. Both peak-to-peak amplitudes and signal integrals were calculated for

all the traces. The graph compares the results obtained with both methods. In both cases, the measured signal from the water sample is subtracted and a linear regression is performed to determine the limit of detection. At the concentrations studied, we assumed the signal depends linearly with concentration due to very low laser energy and the contribution of water was equal for all samples. From both amplitude and integral analysis, similar values on the order of $A=2x10^{-6}$ were obtained. We hypothesized the significant signal generated by the water layer (Fig. 3A, magnitude comparable as that of sample S32 in spite of absorbance 7 times lower) was due to acoustic etaloning within the sample thickness, as 18 μm correspond roughly to the displacement of an acoustic wave within the duration of the laser pulse (12 ns). Extensive thickness-dependent studies are needed to corroborate this observation and explain the phenomenon.

GNR Adsorbed on Acrylic Substrate

While investigating the possibility of furthering the experiment described above by observing optoacoustic signals emanating from solutions of GNR, it has been determined that pegylation of the rods is not sufficient to fully passivate against adsorption onto acrylic surfaces. Therefore, samples were fabricated by adsorbing pegylated GNR onto clean acrylic surfaces. A diluted GNR-PEG solution with optical density approximately 0.03 was prepared. A 200 μL aliquot of the solution was deposited on an acrylic surface and spread over an area of several cm^2, and immediately washed off with copious amounts of milliQ water. Imaging of adsorbed GNR was performed using a custom dark-field microscopy setup. For illumination, we used a dry dark field condenser (Olympus) with NA of 0.7-0.9 mounted under the stage of an inverted microscope (Accu-Scope). A 20X objective was used for light collection. The images were recorded with a thermoelectrically cooled Apogee Alpha U2 CCD camera. Images of the acrylic slide before and after deposition of GNR are shown below (Fig. 4). Similar defects are present on both images, indicating reproducibility in positioning the slide onto the microscope. After GNR deposition, we observe new faint spots which we attribute to scattering from individual GNR. It is possible to count the number of such spots in these images and provide a rough estimate of GNR density on this surface. This analysis yields on the order of 10^5 GNRs per mm^2.

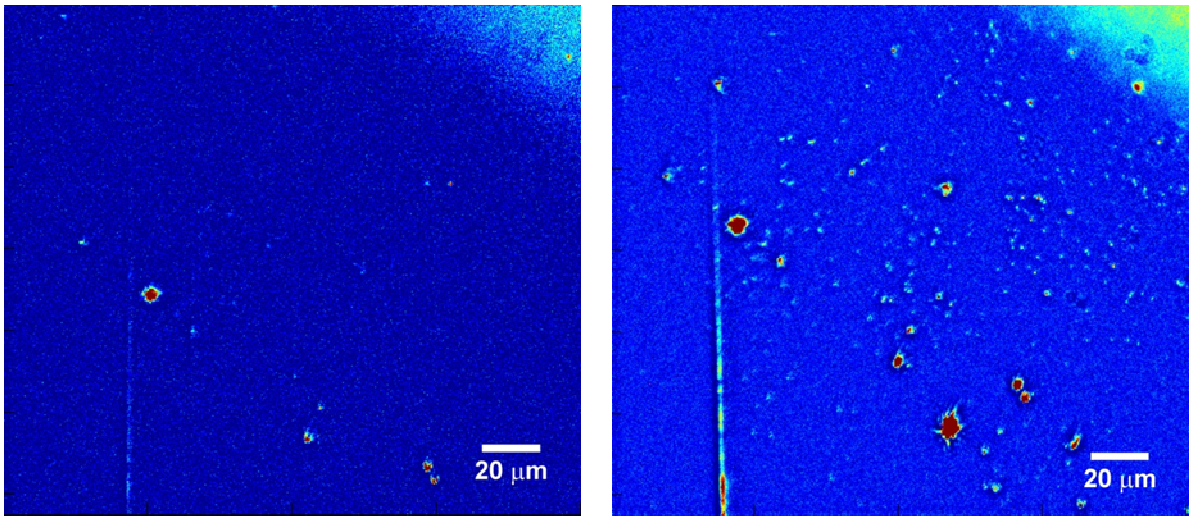

Figure 4. Dark field microscopy images of A) clean acrylic plate and B) acrylic plate coated with minute amount of heavily diluted pegylated GNR solution.

Following microscopy analysis, the slides were interrogated optoacoustically. The slide was deposited, GNR down, onto the top delay line of the detector: about 150 µl of deionized water was first deposited on the detector and used as acoustic couplant. The same laser parameters as in the ionic solutions experiment were used, and the traces were analyzed in a similar fashion (i.e. removal of sloping offset through subtraction of blank data). Two signals, corresponding to two areas of the sample plate, are shown in the graph below (Fig. 5). Since the coating process isn't controlled at this time, the GNR density on the surface varies and the signal therefore varies accordingly (here from about 0.8 to 1.2 mV). Analysis of the signal present in the flat portion of the baseline just before the initial rise shows a noise figure on the order of 85 μV_{RMS}. Both traces show an average amplitude of 1 mV, so we can conclude that a density of 10^5 GNR per mm^2 yields a signal-to-noise ratio of about 10, and correspondingly a noise equivalent power of 10^4 GNR per mm^2.

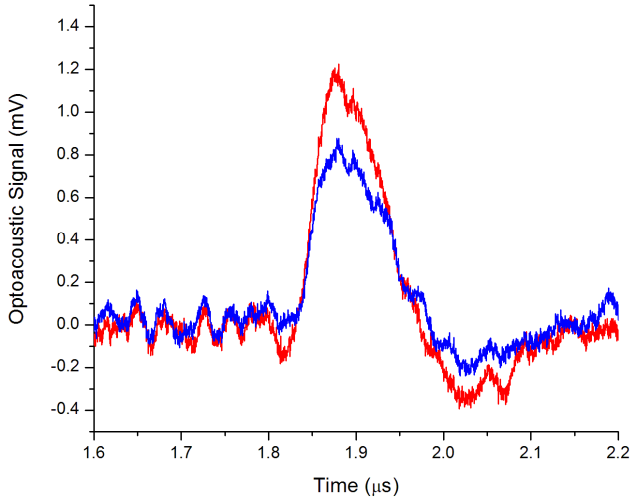

Figure 5. Optoacoustic signals collected from illumination of GNR adsorbed onto an acrylic substrate. Blank scans were subtracted in order to straighten the baseline, unfortunately also increasing experimental noise.

CONCLUSIONS

We have successfully developed an optoacoustic biosensor for the detection of antibody-coupled gold nanorods as a contrast agent. Optoacoustic responses generated by the samples are detected in forward mode using a wide band ultrasonic transducer. The sensitivity of the technique has been determined: Both ionic solutions and gold nanorods served as the contrast agent generating the optoacoustic response. The sensitivity of Nano-LISA is at least $OD=10^{-6}$ which allows reliable detection of GNR solutions of concentration around 2pM. By comparison, the noise equivalent power of standard ELISA detection is on the order of 10 pM. When interrogating samples made of GNR adsorbed on acrylic plates, the noise equivalent power is determined to be about 10^4 GNR per mm^2. Through further improvements aimed at increasing the sensitivity of the method, we believe NanoLISA will prove to be a viable alternative to ELISA as it will yield a faster treatment of biological samples without the need for increasing sample concentration through lengthy viral or bacterial cultures.

REFERENCES

[1] Aloysius, P. and Geraldine, P., "Infectious Keratitis," Curr Opin Infect Dis 20, 129-141 (2007).
[2] Luna, V. A., King, D. and Davis, C., "Novel sample preparation method for safe and rapid detection of bacillus anthracis spores in environmental powders and nasal swabs," J Clin Microbiol 41, 1252-1255 (2003).
[3] Hoffmaster, A. R., Meyer, R. F. and Bowden, M. D., "Evaluation and validation of a real-time polymerase chain reaction assay for rapid identification of bacillus anthracis," Emerg Infect Dis 8, 1178-1182 (2002).
[4] Biagini, R. E., Sammons, D. L. and Smith, J. P., "Comparison of a multiplexed fluorescent covalent microsphere imunoassay and an enzyme-linked immunosorbent assay for measurement of human immunoglobulin G antibodies to anthrax toxins.," Clin Diagn Lab Immunol 11(1), 50-55 (2004).
[5] Biagini, R. E., Sammons, D. L. and Smith, J. P., "Determination of serum IgG antibodies to bacillus anthracis protective antigen in environmental sampling workers using a fluorescent covalent microsphere immunoassay," Occup Environ Med 61(8), 703-708 (2004).
[6] Oraevsky, A. A., Jacques, S. L. and Tittel, F. K., "Measurement of tissue optical properties by time-resolved detection of laser-induced transient stress," Appl. Opt. 36(1), 402-415 (1997).
[7] Pao, Y.-H., [Optoacoustic spectroscopy and detection], Academic Press, New York, xi, 244 p. (1977).
[8] Rosencwaig, A., [Photoacoustics and photoacoustic spectroscopy], John Wiley & Sons, Malabar, FL, (1990).
[9] Zharov, V. P. and Letokhov, V. S., [Laser optoacoustic spectroscopy], Springer-Verlag, Berlin ; New York, x, 327 p. (1986).
[10] Oraevsky, A. A. and Oraevsky, A. N., "Plasmon resonance in ellipsoid nanoparticles," Quantum Electronics 32(1), 79-82 (2002).
[11] Urbanska, K., Romanowska-Dixon, B. and Matuszak, Z., "Indocyanine green as a prospective sensitizer for photodynamic therapy of melanomas," Acta. Biochim. Pol. 49, 387-391 (2002).
[12] Oraevsky, A. A., Karabutov, A. and Savateeva, E. A., "Enhancement of optoacoustic tissue contrast with absorbing nanoparticles," Proc. SPIE 4434, 60-69 (2001).
[13] Andreev, V. G., Karabutov, A. A. and Oraevsky, A. A., "Detection of ultrawide-band ultrasound pulses in optoacoustic tomography," IEEE transactions on ultrasonics, ferroelectrics, and frequency control 50(10), 1383-1390 (2003).
[14] Liopo, A., Conjusteau, A., Konopleva, M., Andreeff, M. and Oraevsky, A., "Photothermal therapy of acute leukemia cells in the near-infrared region using gold nanorods CD-33 conjugates.," Proc. SPIE (submitted), (2011).
[15] Eghtedari, M., Oraevsky, A. A., Copland, J. A., Kotov, N. A., Conjusteau, A. and Motamedi, M., "High sensitivity of in vivo detection of gold nanorods using a laser optoacoustic imaging system," Nano letters 7(7), 1914-1918 (2007).
[16] Chamberland, D. L., Agarwal, A., Kotov, N., Fowlkes, J. B., Carson, P. L. and Wang, X., "Photoacoustic tomography of joints aided by an Etanercept-conjugated gold nanoparticle contrast agent -- an ex vivo preliminary rat study," Nanotechnology 19, 095101 (2008).
[17] Wehry, E. L., [Molecular fluorescence and phosphorescence spectrometry], Prentice-Hall Professional Technical Reference, Upper Saddle River, NJ, 507 (1997).
[18] Eghtedari, M., Liopo, A. V., Copland, J. A., Oraevsky, A. A. and Motamedi, M., "Engineering of Hetero-Functional Gold Nanorods for the in vivo Molecular Targeting of Breast Cancer Cells," Nano letters 9(1), 287-291 (2009).
[19] Sau, T. K. and Murphy, C. J., "Seeded High Yield Synthesis of Short Au Nanorods in Aqueous Solution," Langmuir 20, 6414-6420 (2004).
[20] Eghtedari, M., Oraevsky, A. A., Conjusteau, A., Copland, J. A., Kotov, N. and Motamedi, M., "Functionalized gold nanorods for molecular optoacoustic imaging," Proceedings SPIE 6437, 64370G (2007).
[21] Niidome, T., Yamagata, M., Okamoto, Y., Akiyama, Y., Takahashi, H. and Kawano, T., "PEG-modified gold nanorods with a stealth character for in vivo applications," Journal of Controlled Release 114(3), 343-347 (2006).
[22] Rayavarapu, R. G., Petersen, W., Ungureanu, C., Post, J. N., Van Leeuwen, T. G. and Manohar, S., "Synthesis and bioconjugation of gold nanoparticles as potential molecular probes for light-based imaging techniques.," International Journal of Biomedical Imaging 2007, 29817 (2007).
[23] Maswadi, S. M., Page, L., Woodward, L., Glickman, R.D., Barsalou, N., "Optoacoustic sensing of ocular bacterial antigen using targeted gold nanorods," Proceedings SPIE 6856, 151-158 (2008).

[24] Conjusteau, A., Maswadi, S. M., Ermilov, S. A., Brecht, H. P., Barsalou, N., Glickman, R. D. and Oraevsky, A. A., "Detection of gold-nanorod targeted pathogens using optical and piezoelectric optoacoustic sensors: comparative study," Proceedings SPIE 7177, 71771P (2009).
[25] Conjusteau, A., Ermilov, S. A., Brecht, H. P. and Oraevsky, A. A., "Effects of optical energy distribution on the generation of acoustic plane waves," Proceedings SPIE 7564, 75641L (2010).